Screening of Heterogeneous Photocatalysts for Water Splitting

Michael Schwarze[1,*], Tabea A. Thiel[1,2], Adeem G. Rana[3], Jin Yang[1], Amitava Acharjya[1], Anh Dung Nguyen[1], Simon Tameu Djoko[1], Edith M. Kutorglo[1,4], Minoo Tasbihi[1], Mirjana Minceva[3], Shahana Huseyinova[1,5], Prashanth Menezes[1,6], Carsten Walter[1], Matthias Driess[1], Reinhard Schomäcker[1], and Arne Thomas[1]

DOI: 10.1002/cite.202200070

In this contribution, a simple method for the screening of photocatalytic activity of catalyst materials is presented. The method is based on two steps: the immobilization of the photocatalyst and the subsequent testing of their photocatalytic activity, using the gas evolution at the solid-liquid interface. Up to four catalysts can be tested under the same conditions. The observed gas evolution for selected photocatalysts is consistent with trends reported in the literature from conventional photocatalytic reactors.

Keywords: Hydrogen, Photocatalyst, Screening, Supported catalyst, Water splitting

Received: March 20, 2022; *revised:* July 05, 2022; *accepted:* July 26, 2022

1 Introduction

Concerning a sustainable future energy supply, photocatalytic water splitting is an important field of research [1]. The core of this field is the photocatalyst, a semiconductor material in heterogeneous photocatalysis, where electron-hole pairs are initially generated by light absorption. After this, water molecules are oxidized to oxygen by the holes (OER, oxygen evolution reaction), while the protons are reduced to hydrogen by the electrons (HER, hydrogen evolution reaction). Only a few photocatalysts, e.g., GaN/ZnO [2], fulfill the requirements for overall water splitting, that is, HER and OER catalyzed by the same system. In contrast, many photocatalysts can perform either HER or OER using sacrificial reductants or oxidants [3]. In some cases, two photocatalysts can also be combined into Z-scheme water splitting systems using redox mediators [4, 5]. A Google Scholar search with the keyword "Photocatalyst" shows more than 30 000 entries only for 2021, underlining the high interest in this field [6]. Independent of the type of photocatalytic reaction, various lab-scale experiments must be established to test new photocatalysts and find promising candidates. These experiments can be simple catalyst screenings or detailed kinetic studies of the impact of operating conditions. Most of the catalytic studies on heterogeneous photocatalysis are performed in slurry systems with dispersed photocatalysts using high-energy lamps (e.g., a 300 W Xe lamp) operated on a time scale between 6 and 24 h, whereby successful gas production (O_2, H_2, or H_2/O_2) is verified by gas chromatography. Gas production, thus catalyst performance, depends on a variety of operating conditions such as catalyst concentration, co-catalyst selection and co-catalyst loading, as well as the type and concentration of sacrificial agent. All possible variations thus result in a huge matrix of required experiments to find the optimum conditions for photocatalytic tests. Related to this topic, two main problems can be identified: a) a costly setup (GC ana-

[1]Dr. Michael Schwarze, Tabea A. Thiel, Jin Yang, Amitava Acharjya, Anh Dung Nguyen, Simon Tameu Djoko, Dr. Edith M. Kutorglo, Dr. Minoo Tasbihi, Dr. Shahana Huseyinova, Dr. Prashanth Menezes, Dr. Carsten Walter, Dr. Matthias Driess, Dr. Reinhard Schomäcker, Dr. Arne Thomas
ms@chem.tu-berlin.de
Technische Universität Berlin, Department of Chemistry, Straße des 17. Juni 124, 10623 Berlin, Germany.

[2]Tabea A. Thiel
Leibniz-Institut für Katalyse, Albert-Einstein-Straße 29a, 18059 Rostock, Germany.

[3]Adeem G. Rana, Dr. Mirjana Minceva
Technical University of Munich Weihenstephan, Biothermodynamics, TUM School of Life Sciences, Maximus-von-Imhof-Forum 2, 85354 Freising, Germany.

[4]Dr. Edith M. Kutorglo
University of Chemistry and Technology, Department of Chemical Engineering, Technická 3, 166 28 Prague 6 – Dejvice, Czech Republic.

[5]Dr. Shahana Huseyinova
University of Santiago de Compostela, Department of Chemistry, Avenida do Mestre Mateo 25, 15706 Santiago de Compostela, Spain.

[6]Dr. Prashanth Menezes
Helmholtz-Zentrum Berlin für Materialien und Energie, Materials Chemistry Group for Thin Film Catalysis – CatLab, Albert-Einstein-Straße 15, 12489 Berlin, Germany.

lytics) is needed and b) the experiments are time and energy consuming. In addition, the number of synthesized photocatalysts is often much higher than the available test capacities to investigate them in a reasonable time. To increase competitiveness of photocatalyst development, the time for catalytic testing must be reduced, for which a rapid test method for photocatalysts is desirable so that suitable candidates for further investigations can be identified at an early stage, minimizing time and material input.

This contribution presents a simple, cheap, and fast test facility for photocatalysts in water splitting. The method is based on the fundamental principle of heterogeneously photocatalyzed water splitting and the associated formation of gas (H_2, O_2, or both) at the liquid-solid phase boundary. The whole catalyst screening consists of two steps: a) the immobilization of the powder photocatalyst and b) the observation of gas evolution in the main screening experiment. This new method allows for screening several photocatalysts simultaneously under the same reaction conditions. To validate the screening reactor, the test device was used to investigate the performance of already published photocatalysts under certain operating conditions.

2 Experimental Part

2.1 Modification of Cellulose for Photocatalyst Immobilization

Cellulose, isolated from *styela clava*, was purchased from van den Berg chemicals. The cellulose was modified by sulfuric acid (H_2SO_4, 96 %, Roth) hydrolysis as reported by van den Berg et al. with slight modifications [7]. 4.5 g of cellulose and 120 mL of water were placed into a double-walled glass reactor, and the temperature was set to 4 °C. Under vigorous stirring, 120 mL of H_2SO_4 were added. The temperature was raised to 60 °C, where the mixture was stirred for 2 h before it was cooled down again to 4 °C. The cellulose suspension was filtered using a small-pore sintered-glass filter and washed until the pH was neutral, and finally freeze-dried for three days (Alpha 1-4, Christ). The modified cellulose was abbreviated as ModCe.

2.2 Immobilization of Heterogeneous Powder Photocatalysts

The immobilization of the powder photocatalyst consists of three steps. First, a 5 g L^{-1} ModCe dispersion in a mixture of water (w) and methanol (m) (V_w/V_m = 30/70) was prepared. Secondly, 66 mg of the solid photocatalyst (10 mg for TtaTfa) was mixed with 12.5 mL (8 mL for TtaTfa) of the prepared ModCe dispersion and sonicated to homogenize the catalyst suspension. Finally, the catalyst suspension was vacuum filtered through a common filter paper (diameter = 7 cm) until dryness. The following photocatalysts were immobilized by this method: P25 (Evonik), P90 (Evonik), PC105 (Cristal Global), PC500 (Cristal Global) (all are TiO_2 modifications), PC500 with immobilized platinum nanoparticles (PtNP@PC500), GaN/ZnO, exfoliated carbon nitride with immobilized platinum nanoparticles (PtNP@exf-CN,[8]), mesoporous carbon nitride (mp-CN, [9]), covalent organic framework based on 2,4,6-tris(4-aminophenyl)triazine and tris(4-formyl phenyl)amine (TtaTfa, [10]) without (COF) and with immobilized platinum Nanoparticles (Pt@COF), and WO_3 (Sigma Aldrich, < 100 nm particle size).

2.3 Screening of Photocatalysts

For the screening of the photocatalysts, a homemade setup was used that allows for measuring four photocatalysts simultaneously. The setup will be introduced in detail in Sect. 3.1. For the measurements, a tissue (responsible for liquid absorption and transport) and the immobilized photocatalysts were cut into small pieces with a diameter of 1 cm using a punching iron. The cloth was placed into the test chamber at positions 1 to 4, and the immobilized photocatalyst was placed on the top (Fig. 1d). The reaction medium was placed on top of the immobilized catalyst, and the setup was closed by a quartz glass window. Stripes of the tissue were inserted into the holes in the bottom part of the screening reactor and placed into a Teflon tray (Ø = 10 cm). The reaction medium was added to the tray. After the formation of a thin liquid film between the window and the photocatalyst, a photo was taken. The tray was placed below the selected light source, e.g., 300 W Xe arc lamp (Quantum Design Europe, Germany), UV LED (λ = 365 nm, Neumüller Elektronik GmbH, Germany), VIS LED (λ = 400–800 nm, Bridgelux, United States), or sunlight simulator (Quantum Design Europe, Germany), and irradiated for the desired time. After that, another photo was taken. For evaluation of the catalyst's performance, the photos were compared.

3 Results and Discussion

3.1 Screening Device

Catalyst development is the key to efficient photocatalytic hydrogen production in the future, either by water splitting or water reduction. Many groups worldwide synthesize and test new photocatalysts. The number of catalysts and catalyst variations is continuously increasing. Each reported result is based on a single experiment with defined experimental conditions (e.g., solvent, lamp, time), and analysis is done using a calibrated gas chromatograph. The typical duration for catalyst testing is between 6 and 24 h, which means that the number of catalysts to be tested is limited. New photocatalysts can be tested in series with one setup or

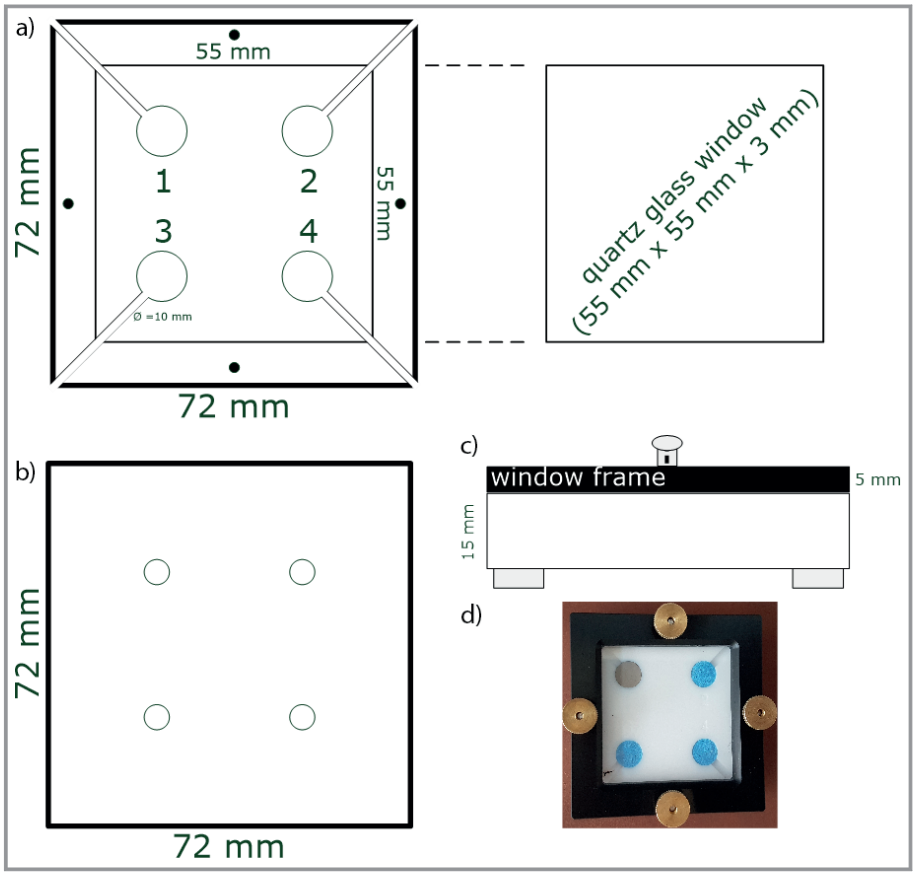

Figure 1. Screening reactor: a) top view, b) bottom view, c) side view, and d) screening reactor with an immobilized PtNP@PC500 photocatalyst on position 1 (a tissue only occupies positions 2–4).

in parallel if several setups are available. The problem is that already one setup requires lab space and money, depending on the individual components. Considering a 300 W Xe arc lamp (with filters), a thermostat (for temperature control), and a glass reactor as the components for a typical photocatalytic setup, the total costs for only one setup will be higher than 20 000 €. The total investment for photocatalytic testing and the number of newly tested photocatalysts will increase with the number of available setups. Additionally, a GC is needed for the analysis of the gas phase. A screening reactor (Fig. 1) was developed in order to identify very active catalysts at an early stage and also to enable rapid testing by all research groups. Photocatalysts with known activity were used to test the new screening reactor as a benchmark.

The screening reactor is constructed from Teflon with positions to simultaneously test four photocatalysts (Fig. 1a, positions 1–4). Quartz glass is selected as window material so UV and visible light can be used in photocatalytic experiments. The advantage of the setup is its simplicity and scalability. More catalysts can be investigated with a suitable light source (the diameter of the light cone must fit the test device) or smaller test samples. For the test examples, it was decided to work with immobilized photocatalysts rather than photocatalyst powders. The photocatalyst films are more suitable for the measurement principle. A recently developed immobilization technique can easily prepare homogeneous photocatalyst films (Sect. 3.2). However, before explaining the measurement principle, it should be noted that the screening reactor allows for the fast qualification of promising photocatalysts for further investigation rather than determining the absolute activity of a material.

The measurement principle is simple and based on the observation of the gas production at the solid-liquid interphase. At first, a small piece of tissue is placed into the deepening at positions 1–4. Afterward, a piece of the immobilized photocatalyst with the same diameter as the cloth is placed on top. The next step is the addition of the solvent (water or a sacrificial agent solution). The first idea was to transport the liquid from an outer reservoir through the tissue placed into the holes in the bottom (Fig. 1b). As shown in Fig. 2, this works in principle.

However, it is difficult to exclude air between the sample and the glass plate, which would cause problems in interpreting the images. Therefore, it was decided to place the liquid directly on top of the immobilized photocatalyst (Fig. 3b) and close the setup with the quartz glass window (Fig. 3c). In this case, air entrapment can be avoided.

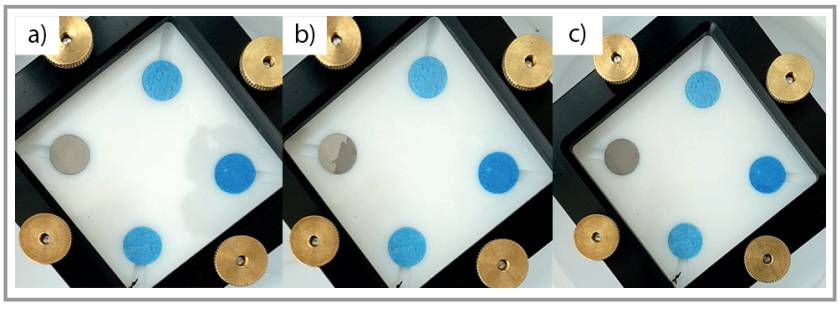

Figure 2. Liquid from the reservoir (a), partially wetted immobilized photocatalyst (b), and fully wetted photocatalyst (c).

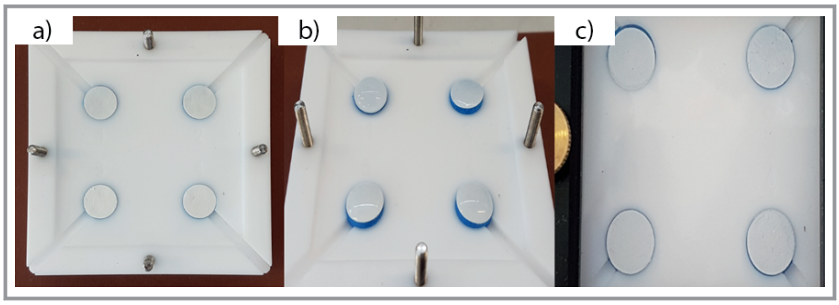

Figure 3. Placed TiO_2 samples (a), added sacrificial agent solution (b), and after closing the reactor with the quartz glass window (c).

Further sacrificial agents during irradiation can be delivered from the reservoir.

After the immobilized film is wetted, a photo is taken, and the sample is irradiated. When the sample is active for gas evolution, the gas production becomes visible through voids in the liquid film (Fig. 4). Fig. 4a shows the surface of immobilized PtNP@PC500. The catalyst was irradiated for about 35 min with a solar simulator using ethanol as the sacrificial agent. The sample is very active, producing a significant gas amount (Fig. 4b).

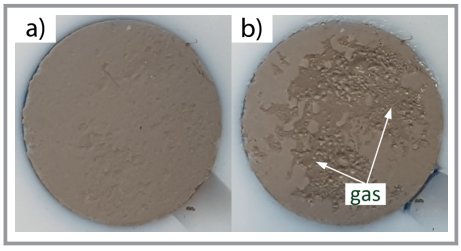

Figure 4. The surface of PtNP@PC500 before (a) and after (b) irradiation with a solar simulator for 35 min (SA = EtOH, 10 % in H_2O).

The screening reactor can be used to investigate most of the standard reaction parameters such as light source, sacrificial agent, and co-catalyst. When the images before and after irradiation are taken under the same conditions (distance, focus, and illumination), the catalyst's activity can be further evaluated using imaging software. It is also possible to take videos of the gas evolution, if the camera can compensate for the high luminous intensity of some lamps. After identifying a promising catalyst, further experiments to determine the H_2 production rate or the composition of the gas phase can be done as usual.

It is important to emphasize that we aimed for an easy and cheap method to screen photocatalysts. The highly complex photocatalytic system is broken down to the basics, the observation of gas production. The setup will identify the most active catalyst even without knowing the full rate. A more detailed and expensive high-throughput screening device, including full analysis based on computation and robotics, is shown by Bai et al. [11]. The parallelization of reactors, together with automated analysis, by time-shifted sample application, is a well-known approach derived from homogeneous catalysis [12].

3.2 Photocatalyst Immobilization

In heterogeneous photocatalysis, the photocatalyst is usually present as a solid powdered material, investigated as suspension. To measure several powder photocatalysts simultaneously, the immobilization of the powder as a thin film is better. In this case, all catalysts can be measured in only one setup, lowering costs. The techniques for film preparation are manifold, drop coating, spin coating, electrodeposition, chemical vapor deposition, or sol-gel deposition are only a few often used examples [13–15]. These techniques are quite time-consuming and sometimes require special conditions or auxiliaries. As part of the photocatalyst screening, the immobilization should be easy, fast, and reproducible. Recently, a method was developed for photocatalyst immobilization based on cellulose as a binder [16, 17]. There are two possibilities for immobilization: a) the photocatalyst is immobilized on the surface of a filter paper with cellulose, and b) the photocatalyst and the cellulose form a composite membrane. In both cases, the self-aggregation properties of cellulose when removing the solvent are used to form a thin film of the photocatalyst particles with nanocellulose acting as a natural glue. The immobilization method, which consists of three steps, is simple, cheap, and fast. The first step is the preparation of a cellulose suspension, followed by the preparation of a photocatalyst/cellulose suspension as the second step. The third step is the filtration of the suspension until dryness. As cellulose is generally not dispersible in polar solvents like water or methanol, it was treated with sulfuric acid as described in the experimental part. Such an immobilized photocatalyst is active, e.g., for hydrogen production via water splitting [16] or photocatalytic hydrogenation of acetophenone [17].

For the screening experiments, all selected photocatalysts were immobilized on the surface of a filter paper. In most cases, the successful immobilization is obvious from the surface color (Fig. 5). The filter paper is colorless (Fig. 5a), whereby after immobilization of, e.g., mp-CN (Fig. 5b) or WO_3 (Fig. 5j), the surface color changes to orange and light green, respectively.

As additional proof, the immobilization was verified by XRD measurements. Fig. 6 shows the XRD pattern of six immobilized photocatalysts. All signals were normalized to the strongest cellulose peak (about 22.5°). Except for TtaTfa, the amount of photocatalyst and cellulose during immobilization onto the filter paper (Ø = 7 cm, A = 38.5 cm^2) was 66 mg and 62.5 mg, respectively.

The pure filter paper shows four characteristic 2Θ reflection peaks at 14.5°, 16.5°, 22.5°, and 35°, which are typical

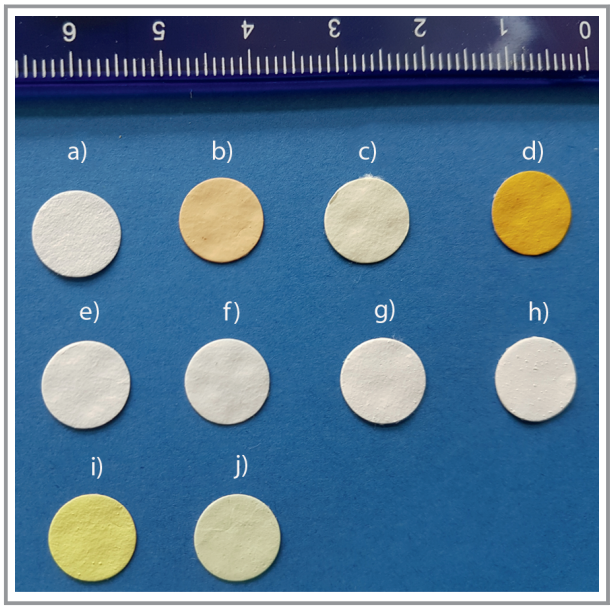

Figure 5. Selected immobilized photocatalysts: a) pure filter paper, b) mp-CN, c) Pt@exf-CN, d) TtaTfa, e) P25, f) P90, g) PC105, h) PC500, i) GaN/ZnO, and j) WO_3.

for cellulosic materials [18]. These four peaks are shown in all immobilized photocatalysts. Further, each sample shows the characteristic peaks of the photocatalyst powder. The two carbon nitride photocatalysts, mp-CN and Pt@exf-CN show a peak at about 27.4°, corresponding to the (002) plane [9, 19]. Although the exf-CN is covered with Pt, the concentration is too low to show a peak in XRD. The COF TtaTfa shows a small signal at about 11.5°, which has been reported [10]. There are more signals for TtaTfa, but some overlap with the cellulose peaks (about 15°) or are not shown (below 10°). As the mass of COF during the immobilization was lower than that of other catalysts, the one reflection peak was small. WO_3 shows several reflection peaks at about 23.1°, 23.6°, 24.3°, 26.5°, 28.8°, 41.8°, and 50°, which correspond to the (002), (020), (200), (120), (112), (222), and (232) planes of monoclinic WO_3 [20]. The GaN/ZnO photocatalyst has five characteristic peaks in the 2Θ range of 30–60°, as shown by Wang et al. [21]. Except for one peak that overlaps with the cellulose peak (about 35°, corresponds to the (002) plane), all peaks are clearly seen. The other peaks of GaN/ZnO are at about 32°, 36.5°, 48°, and 57.5°. The TiO_2 modification P25 consists of anatase and rutile phases, and peaks for both phases are shown for the immobilized P25 in XRD. The peak at about 27.5° belongs to the (110) plane of the rutile phase. The peaks at about 25°, 38°, 48°, 54, and 55.2° belong to the (101), (004), (200), (105), and (211) planes of the anatase phase [22].

The photocatalysts have been immobilized because photocatalyst films are easier to measure in the device than photocatalyst powders. When immobilizing a photocatalyst, the photocatalytic activity of the film is lower than the activity of the suspended photocatalyst. However, when all photocatalysts are immobilized with the same method and conditions, their films are expected to show the same catalytic activity trend as the powders. Even though we decided to use a method based on cellulose to prepare the films, many other methods could be used. It is only important that after immobilization, the liquid phase stays in contact with the photocatalyst's surface.

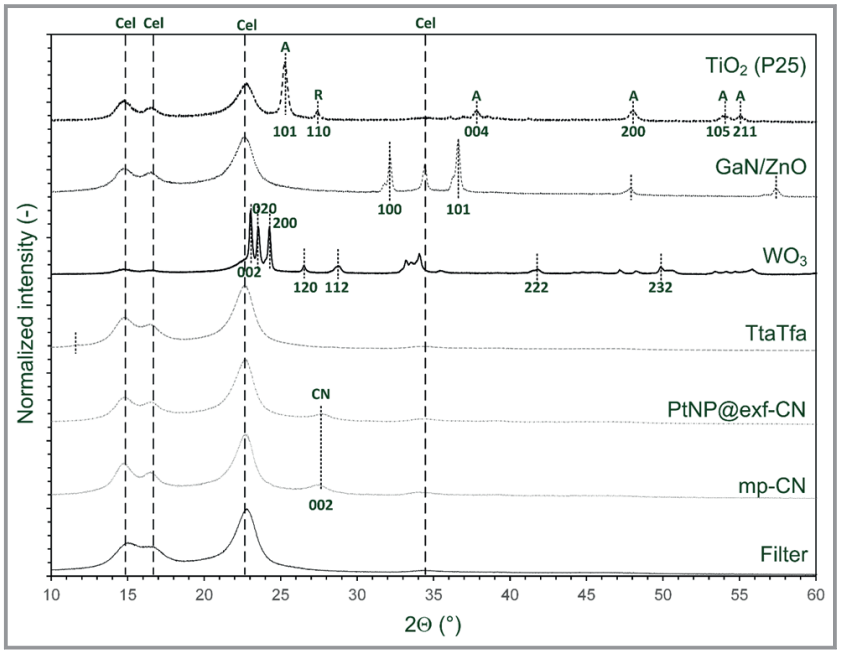

Figure 6. XRD pattern of filter paper and selected immobilized photocatalysts (Cel = cellulose).

3.3 Photocatalyst Screening

In typical test devices with suspended photocatalysts, the reaction conditions, e.g., the selected light source, will influence the activity and the produced amount of gas. Fig. 5 shows several successful immobilized photocatalysts that are known for water splitting. For the screening experiments, photocatalysts were selected for studying trends in photocatalytic hydrogen production. Therefore, photocatalysts with different properties, e.g., with different bandgap energies (BGE) or being modified with Pt nanoparticles as the co-catalyst, have been selected to test the performance of the screening reactor. Based on the experimental conditions, significant differences should be obtained in the

screening reactor according to their properties. Two basic types of catalysts have been selected: a) titanium dioxide (BGE = 3.0–3.2 eV) and b) C,N-based materials (carbon nitride (BGE = 2.7 eV) and COF).

TiO_2 is the most investigated semiconductor photocatalyst and is available in many modifications. The main differences are in the crystal structure and surface area. Four modifications were selected for the investigations, namely P25, P90, PC105, and PC500. P25 is a mixture of rutile and anatase phases with a surface area of about 56 m^2g^{-1}. P90 is also a mixture of anatase and rutile phases but has a higher surface area of about 104 m^2g^{-1}. PC105 and PC500 consist only of the anatase phase with surface areas of 80 and 270 m^2g^{-1}, respectively [23]. As TiO_2 has a large bandgap energy, photocatalytic hydrogen production from water can only take place under UV irradiation. As the four commercial TiO_2 photocatalysts significantly differ in their material properties, they are expected to have different photocatalytic activity when irradiated with UV light. Further, they should not produce hydrogen in the absence of UV light. Therefore, two experiments were carried out: a) simultaneous irradiation with a 365 nm UV LED and b) simultaneous irradiation with a visible light LED (400–800 nm). The four types of TiO_2 were immobilized as described, shown in Fig. 5e–h. After the immobilization, the surface of all catalysts is white, but during UV irradiation with ethanol as the sacrificial agent, the color changes to blue. This change is due to trapped electrons and the formation of Ti^{3+} active sites [24, 25]. After switching off the UV LED, the catalyst is reoxidized, and the color changes back to white. Fig. 7 shows the immobilized catalysts before and after 60 min UV irradiation. The PC500 photocatalyst obviously outperforms the other three types. Many voids due to the produced gas bubbles can be detected. P25 shows the lowest activity. P90 and PC105 have a higher activity than P25 but lower than PC500. Recently, Schwarze et al. [23] investigated photocatalytic hydrogen production with the same TiO_2 photocatalysts using the full spectrum of a 300 W Xe lamp. They obtained the following order for the activity: PC500 > P105 ≈ P90 > P25. Every single experiment was carried out for three hours, so the time to test all four commercial TiO_2 photocatalysts was about 20 h (including GC measurement, cleaning, etc.). The same order in catalytic activity was observed with the new screening setup. The most active type of TiO_2 was identified in a single experiment taking only one hour. When the UV-LED was replaced by the VIS-LED, no significant activity was observed because, for the high bandgap energy of TiO_2, UV light is required.

In the next step, the impact of the co-catalyst was studied. In literature, most photocatalysts use *in-situ* deposited Pt nanoparticles as the co-catalyst. Therefore, Pt was selected as the co-catalyst for PC500, too. However, the screening method requires ex-situ Pt immobilization, which can be done using different techniques, e.g., photodeposition or impregnation [26]. Fig. 8 shows the impact of the co-catalyst. PC500 with Pt as the co-catalyst (Fig. 8b) is more active than PC500 (Fig. 8a). After 10 min UV irradiation, gas production is observed in the image (Fig. 8d). The co-catalyst loading for different photocatalysts should be similar for a better comparison. Suppose different techniques are used for co-catalyst deposition. In that case, it is expected that the differences in loading, dispersion, and size of the nano-

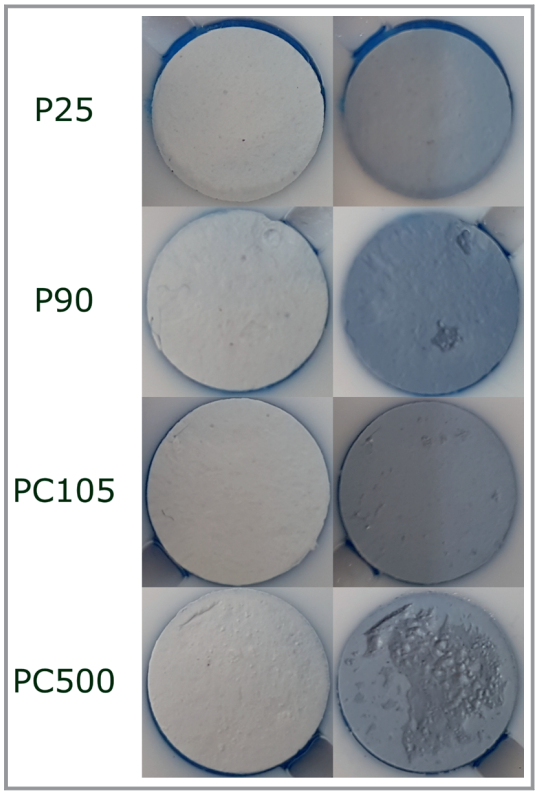

Figure 7. Immobilized commercial TiO_2 photocatalysts before (left) and after 1h UV (λ = 365 nm) irradiation (right) (SA = EtOH, 10 % in H_2O).

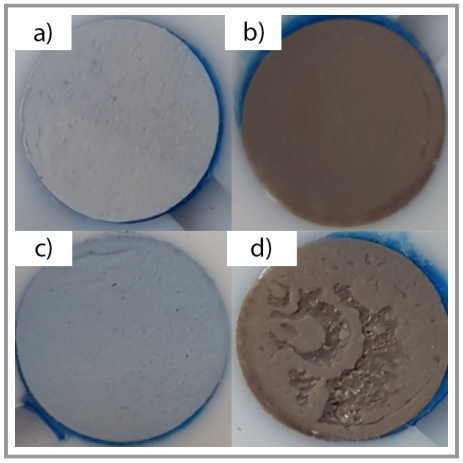

Figure 8. PC500 and Pt@PC500 before (a, b) and after 10 min UV-LED irradiation (c, d) (SA = EtOH, 10 % in H_2O).

particles will lead to different gas production activities so that the best deposition method/conditions will lead to the most active photocatalyst.

A similar set of experiments was performed with C,N-based photocatalysts. As test samples, mesoporous carbon nitride, exfoliated carbon nitride with Pt, and the COF TtaTfa were used. When using triethanolamine (TEOA) as the sacrificial agent in combination with a solar simulator as the light source, the following order was observed Pt@exf-CN > mp-CN / COF. It is known that TEOA is the most suitable sacrificial agent for carbon nitride photocatalysts and Pt, as shown in Fig. 8, increases the activity significantly. Therefore, this order is meaningful and agrees well with the literature. The COF material is not active with TEAO, as reported by Yang et al. [10]. When using ascorbic acid as the sacrificial agent and Pt as the co-catalyst, the COF material outperforms the carbon nitride photocatalysts, as shown in Fig. 9d. After 30 min irradiation with the sunlight simulator, a huge amount of produced gas is observed, indicating the high activity of the COF material under the selected conditions.

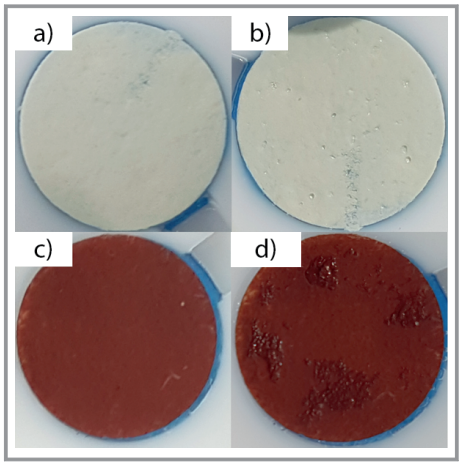

Figure 9. Pt@exf-CN and Pt@COF before (a, c) and after 30 min solar simulator irradiation (b, d) (SA = ascorbic acid, 0.1 M).

In the examples shown, only one sacrificial agent was ever used, e.g., ethanol in the case of TiO_2 or triethanolamine for the carbon nitrides. The selection of the sacrificial agents is based on previous experience and published data. However, the activity of a photocatalyst for the hydrogen evolution reaction only can depend very strongly on the sacrificial agent, as can be seen from the example of COF, where ascorbic acid has so far shown the best performance. With the help of the screening reactor, it is also possible to test the catalyst simultaneously with different sacrificial agents. As shown in Fig. 3, it is sufficient to place a small amount of the sacrificial agent on the immobilized photocatalyst, but it is no longer possible to add more liquid from the reservoir. To give just one example, Pt@COF and Pt@ex-CN, which require ascorbic acid and triethanolamine as an operating reagent, could be measured simultaneously with the same light source.

4 Conclusion

A screening reactor was developed to study the performance of water-splitting photocatalysts simultaneously under the same reaction conditions. At first, the selected photocatalysts were immobilized onto a filter paper using a fast and simple method based on cellulose. The change in surface color and the characteristic XRD pattern are proof of successful immobilization. Secondly, the photocatalytic performance of the immobilized photocatalysts was studied under various conditions and evaluated from the observed gas formation at the solid-liquid interphase. The observed trends, e.g., for different TiO_2 or C,N-based Photocatalysts, are consistent with both expectations and previously published data. Even though the absolute hydrogen production rates were not recorded, the published trends and the expected dependencies could be determined in a much shorter time. The current module is the first prototype and allows the testing of four photocatalysts. However, a model that simultaneously measures a larger number of samples is also possible, either by using a larger light cone or smaller test sizes (< 1 cm). The major challenge is to set a defined initial condition without air entrapment between the sample and the window so that the interpretation of the images and the associated activity is unambiguous. If this condition and also a uniform image quality can be ensured, further evaluation using image processing software is conceivable.

All authors acknowledge support from the Deutsche Forschungsgemeinschaft (DFG, German Research Foundation) under Germany's Excellence Strategy – EXC 2008/1 (UniSysCat) – 390540038. A. N and S. H acknowledges support from the European Union's Horizon 2020 Research and Innovation Program (Bac-To-Fuel 825999), P. W. M. greatly acknowledges support from the German Federal Ministry of Education and Research in the framework of the project Catlab (03EW0015A/B). E. M. K. is grateful to the European Structural and Investment Funds, OP RDE-funded project "CHEMFELLS IV" (No. CZ.02.2.69/0.0/0.0/20_079/0017899) for support. We thank Dr. Michael Schroeter for providing the cellulose. Open access funding enabled and organized by Projekt DEAL.

Sub- and Superscripts

w	Water
m	Methanol

Abbreviations

BGE	Band-gap energy
CEL	Cellulose
CN	Carbon nitride
COF	Covalent organic framework
Exf	Exfoliated
EtOH	Ethanol
GaN	Gallium nitride
GC	Gas chromatography / - chromatograph
H_2	Hydrogen
HER	Hydrogen evolution reaction
LED	Light emitting diode
ModCe	Modified cellulose
O_2	Oxygen
OER	Oxygen evolution reaction
Pt	Platinum
PtNP	Platinum nanoparticles
SA	Sacrificial agent
TEOA	Triethanolamine
TiO_2	Titanium dioxide
UV	Ultra violet
VIS	Visible
Xe	Xenon
ZnO	Zinc oxide

References

[1] N. Fajrina, M. Tahir, *Int. J. Hydrogen Energy.* **2019**, *44 (2)*, 540–577. DOI: https://doi.org/10.1016/j.ijhydene.2018.10.200

[2] K. Maeda, K. Domen, *Chem. Mater.* **2010**, *22 (3)*, 612–623. DOI: https://doi.org/10.1021/cm901917a

[3] A. Kudo, Y. Miseki, *Chem. Soc. Rev.* **2009**, *38 (1)*, 253–278. DOI: https://doi.org/10.1039/b800489g

[4] K. Maeda, *ACS Catal.* **2013**, *3 (7)*, 1486–1503. DOI: https://doi.org/10.1021/cs4002089

[5] A. Kudo, *MRS Bull.* **2011**, *36 (1)*, 32–38. DOI: https://doi.org/10.1557/mrs.2010.3

[6] X. Zou, Y. Zhang, *Chem. Soc. Rev.* **2015**, *44 (15)*, 5148–5180. DOI: https://doi.org/10.1039/C4CS00448E

[7] O. van den Berg, J. R. Capadona, C. Weder, *Biomacromolecules* **2007**, *8 (4)*, 1353–1357. DOI: https://doi.org/10.1021/bm061104q

[8] A. G. Rana, M. Tasbihi, M. Schwarze, M. Minceva, *Catalysts* **2021**, *11 (6)*, 662. DOI: https://doi.org/10.3390/catal11060662

[9] K. Kailasam, J. D. Epping, A. Thomas, S. Losse, H. Junge, *Energy Environ. Sci.* **2011**, *4 (11)*, 4668–4674. DOI: https://doi.org/10.1039/c1ee02165f

[10] J. Yang et al., *Angew. Chemie Int. Ed.* **2021**, *60 (36)*, 19797–19803. DOI: https://doi.org/10.1002/anie.202104870

[11] Y. Bai, L. Wilbraham, B. J. Slater, M. A. Zwijnenburg, R. S. Sprick, A. I. Cooper, *J. Am. Chem. Soc.* **2019**, *141 (22)*, 9063–9071. DOI: https://doi.org/10.1021/jacs.9b03591

[12] J. G. de Vries, A. H. M. de Vries, *European J. Org. Chem.* **2003**, *2003 (5)*, 799–811. DOI: https://doi.org/10.1002/ejoc.200390122

[13] C. Guizard, A. Princivalle, *Catal. Today* **2009**, *146 (3–4)*, 367–377. DOI: https://doi.org/10.1016/j.cattod.2009.05.012

[14] S. Mehla, J. Das, D. Jampaiah, S. Periasamy, A. Nafady, S. K. Bhargava, *Catal. Sci. Technol.* **2019**, *9 (14)*, 3582–3602. DOI: https://doi.org/10.1039/C9CY00518H

[15] M. Stoian, T. Maurer, S. Lamri, I. Fechete, *Catalysts* **2021**, *11 (12)*, 1530. DOI: https://doi.org/10.3390/catal11121530

[16] M. Schwarze, T. A. Thiel, M. Tasbihi, M. Schroeter, P. W. Menezes, C. Walter, M. Driess, R. Schomäcker, *Energy Technol.* **2022**, *10 (1)*, 2100525. DOI: https://doi.org/10.1002/ente.202100525

[17] T. A. Thiel, K. Obata, F. F. Abdi, R. van de Krol, R. Schomäcker, M. Schwarze, *RSC Adv.* **2022**, *12 (12)*, 7055–7065. DOI: https://doi.org/10.1039/D1RA09294D

[18] A. D. French, *Cellulose* **2014**, *21 (2)*, 885–896. DOI: https://doi.org/10.1007/s10570-013-0030-4

[19] S. Y. Tameu Djoko, H. Bashiri, E. T. Njoyim, M. Arabameri, S. Djepang, A. K. Tamo, S. Laminsi, M. Tasbihi, M. Schwarze, R. Schomäcker, *J. Photochem. Photobiol. A Chem.* **2020**, *398*, 112596. DOI: https://doi.org/10.1016/j.jphotochem.2020.112596

[20] R. Hatel, M. Baitoul, *J. Phys. Conf. Ser.* **2019**, *1292 (1)*, 012014. DOI: https://doi.org/10.1088/1742-6596/1292/1/012014

[21] L. Wang, S. Ouyang, B. Ren, J. Ye, D. Wang, *APL Mater.* **2015**, *3 (10)*, 104414. DOI: https://doi.org/10.1063/1.4928702

[22] S. M. C. Rosa, A. B. S. Nossol, E. Nossol, A. J. G. Zarbin, P. G. Peralta-Zamora, *J. Braz. Chem. Soc.* **2016**, *28 (4)*, 582–588. DOI: https://doi.org/10.5935/0103-5053.20160201

[23] M. Schwarze, C. Klingbeil, H. U. Do, E. M. Kutorglo, R. Y. Parapat, M. Tasbihi, *Catalysts* **2021**, *11 (9)*, 1027. DOI: https://doi.org/10.3390/catal11091027

[24] S. Kohtani, E. Yoshioka, K. Saito, A. Kudo, H. Miyabe, *J. Phys. Chem. C.* **2012**, *116 (33)*, 17705–17713. DOI: https://doi.org/10.1021/jp3056174

[25] Z. Xiu, M. Guo, T. Zhao, K. Pan, Z. Xing, Z. Li, W. Zhou, *Chem. Eng. J.* **2020**, *382*, 123011. DOI: https://doi.org/10.1016/j.cej.2019.123011

[26] B. A. T. Mehrabadi, S. Eskandari, U. Khan, R. D. White, J. R. Regalbuto, *Adv. Cat.* **2017**, *61*, 1–35.

